VIII. Detectors and Cosmology

1. Introduction 2

2. CMB Experiments 3

3. Examples of Existing CMB Arrays

MAXIMA 5

SuZIE 8

4. Cryogenic Detector Arrays 12

Detector Sensitivity 13

Thermal Detectors 16

Noise Optimization 19

Heat Capacity 21

Signal Fluctuations 22

Voltage-Biased Transition Edge Sensors 25

Monolithic Fabrication of TES Arrays 31

Readout 36

Signal Summing Schemes 38

Cross Talk 40

Demodulation 42

Some Challenges 44

5. Summary 48

6. Outlook 49

VIII. Detectors and Cosmology

1. Introduction

Recent results from experimental cosmology have raised some profound questions.

Measurements of the Cosmic Microwave Background have shown that the universe if flat.

Measurements of the velocity vs. distance of supernovae indicate that the universe is not just expanding, but that the expansion is accelerating.

$\Rightarrow$ "dark energy" or "dark force"

Best fit to data from BOOMERANG, MAXIMA and DASI indicate

- non-zero cosmological constant
- flat universe with energy density of 0.7 and a matter density of 0.3

These data also reflect tremendous improvements in detector technology.

Automated supernova searches as well as mapping the large-scale structure rely crucially on CCD cameras.

CMB measurements have benefited from ever increasing detection sensitivity.

In this section I will discuss large-scale bolometer arrays for next generation CMB experiments.

2. CMB Experiments

a) Polarization of Cosmic Microwave Background

⇒ POLARBEAR
(A.T. Lee, P. Richards, W. Holzapfel, H. Spieler)

Measure thermal noise from Big Bang

non-isotropic ⇒ matter distribution non-isotropic
⇒ structure in universe

Thomson scattering of CMB photons from electrons

⇒ net polarization of CMB radiation

Potentially provides information on

- surface dynamics at time of last scattering
  (~300,000 years after Big Bang)
- probe gravity waves from inflationary epoch
  (~10^{-38} s after Big Bang)

  gravity waves ⇒ sky patterns with non-zero curl

Could provide irrefutable signature of inflation.

b) Sunyaev Zel'dovich Measurements (W. Holzapfel, et al.)

Inverse Compton scattering

Hot gas bound to clusters of galaxies scatters CMB

$\Rightarrow$ distorts black-body spectrum

$\Rightarrow$ measure motion of galaxies relative to CMB rest frame

Probe of "Dark Energy" - complementary to SNAP

Source counts of distant SZ clusters are a sensitive probe of the epoch at which clusters formed.

Measurements in 100 – 300 GHz range with μK sensitivity.

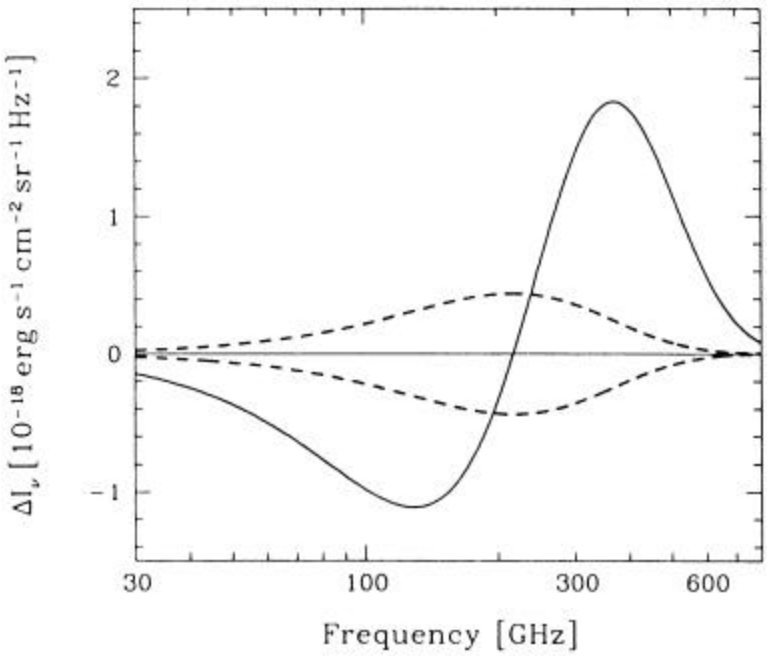

(Holzapfel et al.)

Static SZ effect shifts spectrum (solid line)

Kinetic SZ effect depends on cluster velocity
(dashed curves for positive and negative relative velocity)

Future CMB and SZ measurements require massive step-up in sensitivity

$\Rightarrow$ **large detector arrays**

3. Examples of Existing CMB Arrays

1. Maxima (P. Richards et al.)

Balloon-based experiment (launched in Texas)

Measure angular distribution of temperature variations

Gondola prior to launch

Detector Array

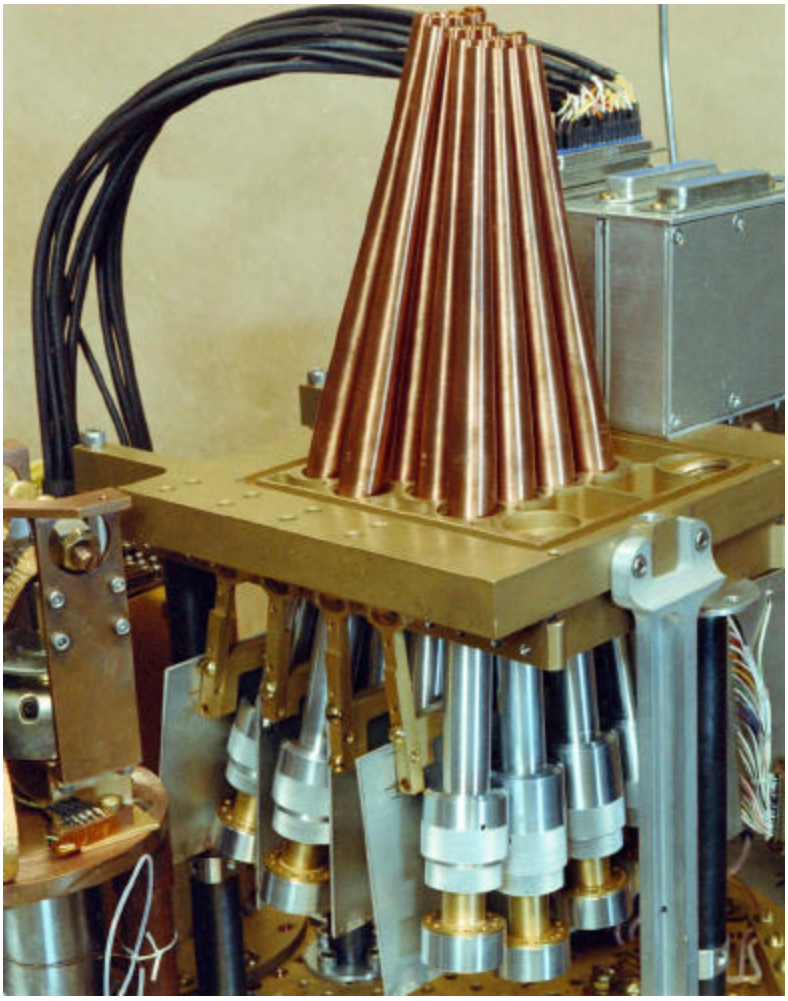

Array of 16 horn antennas coupled to individual bolometers at 100 mK.

Angular resolution: 10’ FWHM

Frequency bands: 150, 240 and 410 GHz (~30 – 60 GHz BW)

Sensitivity: ~100 mK/$\sqrt{\text{Hz}}$

Measure angular distribution of temperature fluctuations and plot vs. multipole

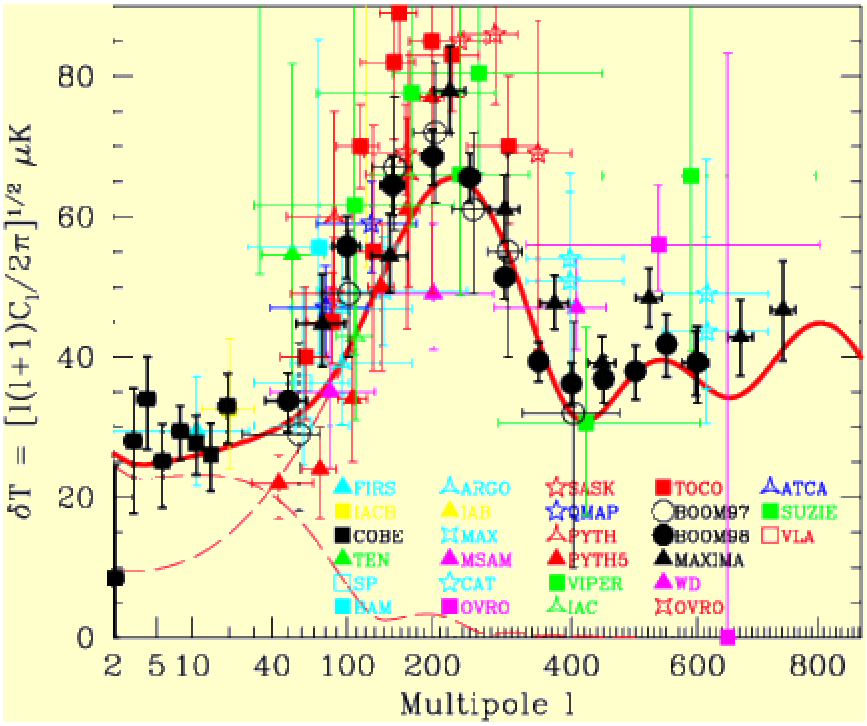

Position of first peak indicates flat universe.

2. SuZIE

W.L. Holzapfel et al., ApJ **479** (1997) 17

Sunyaev-Zeldovich Experiment

Measure at 143, 217, and 269 GHz

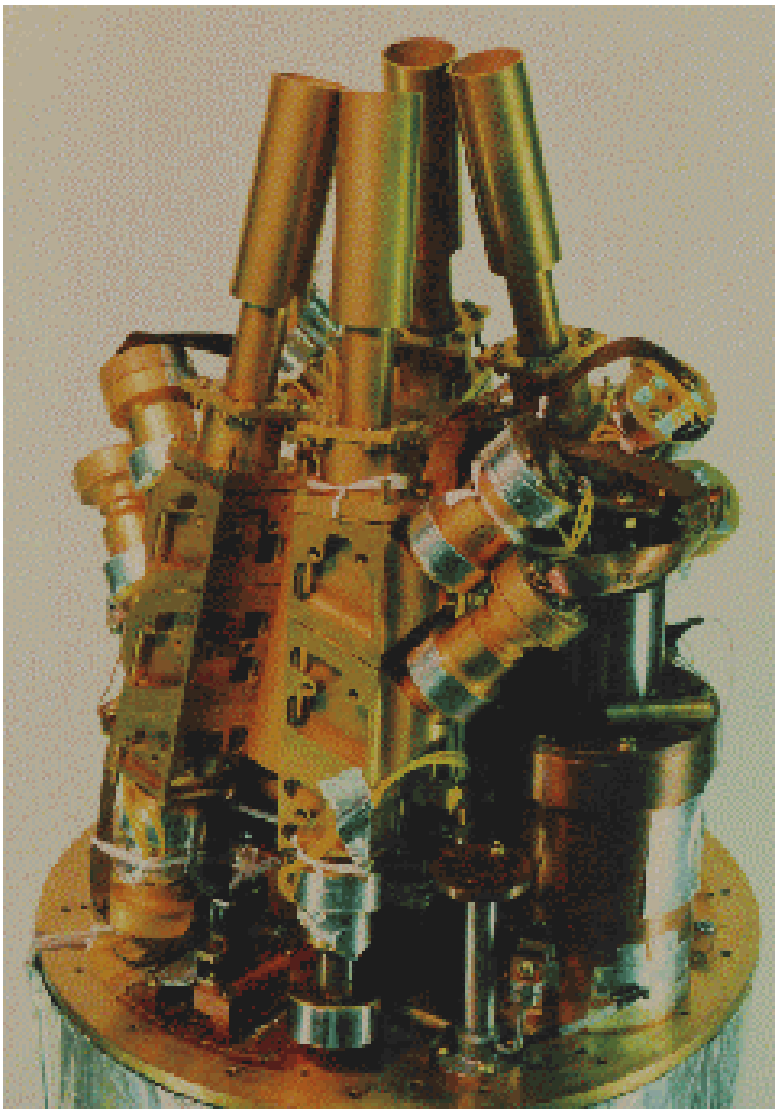

Installed at Caltech Submillimeter Observatory on Mauna Kea

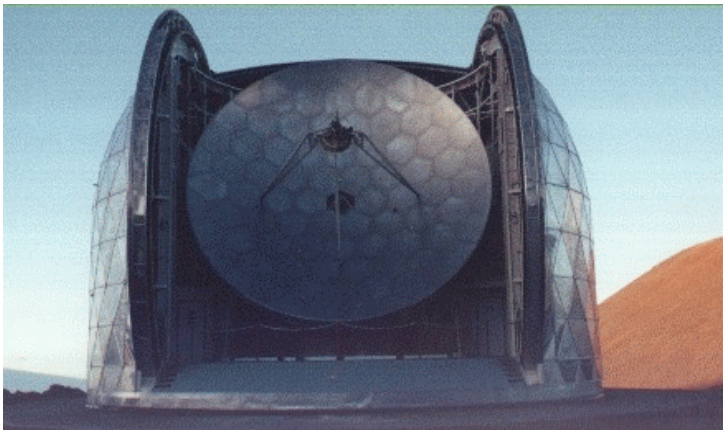

ACBAR Array (Holzapfel et al.)

Deployed at South Pole

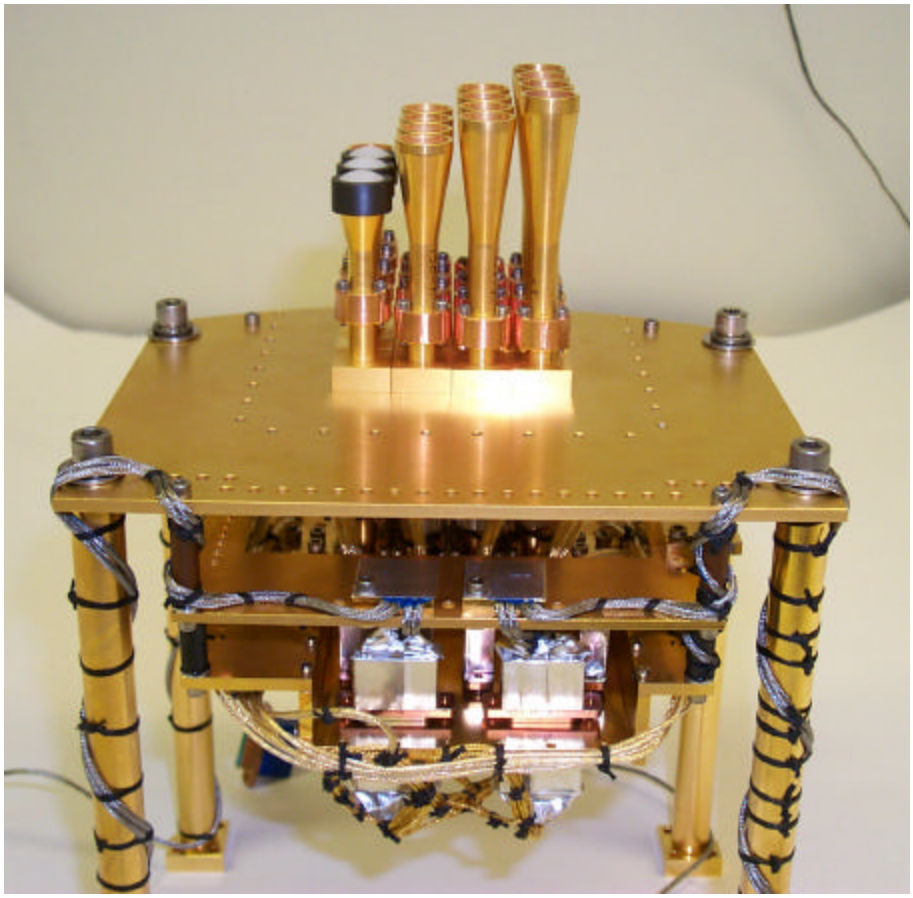

Layout of SuZIE array in CSO Telescope

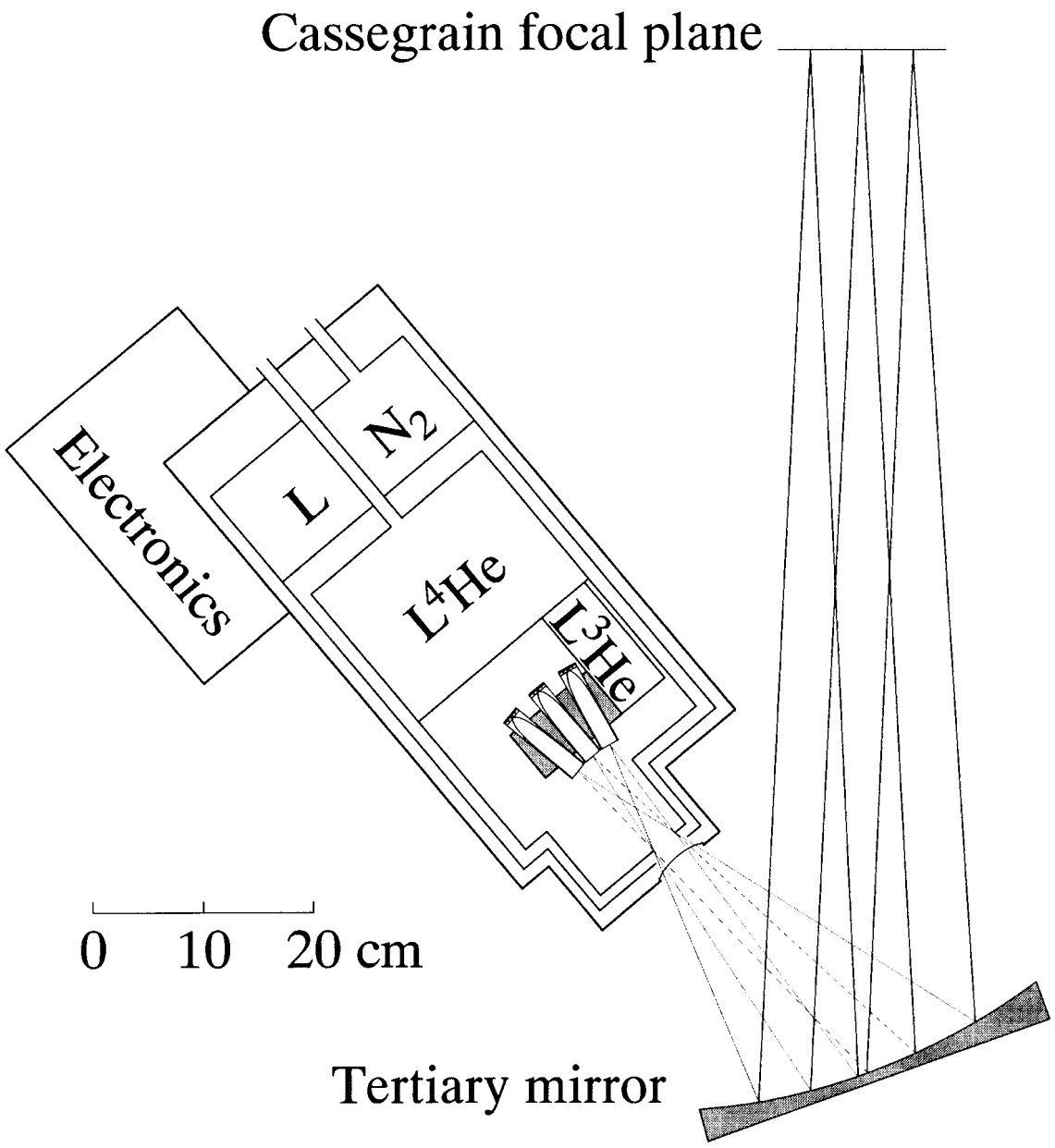

(Holzapfel et al.)

SZ Spectrum measured by SuZIE

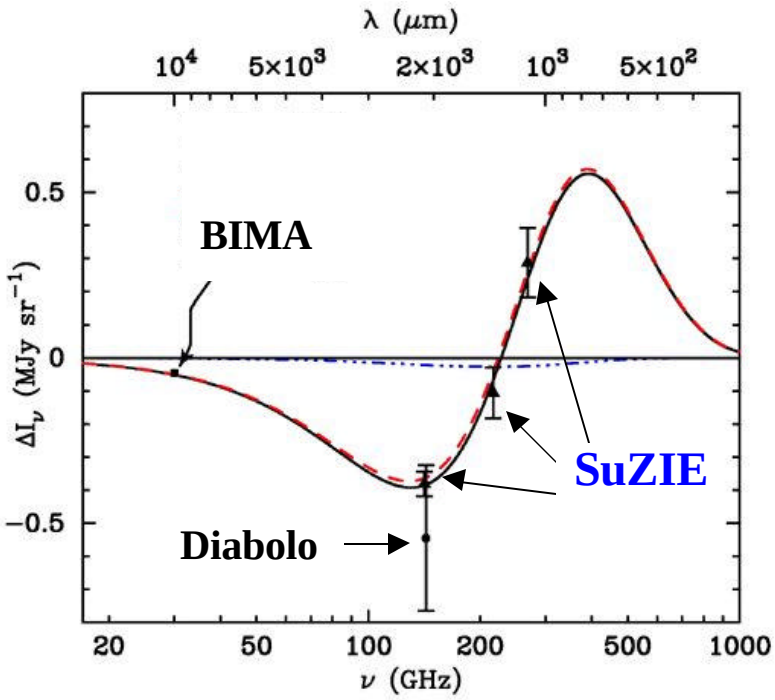

SZ effect independent of redshift

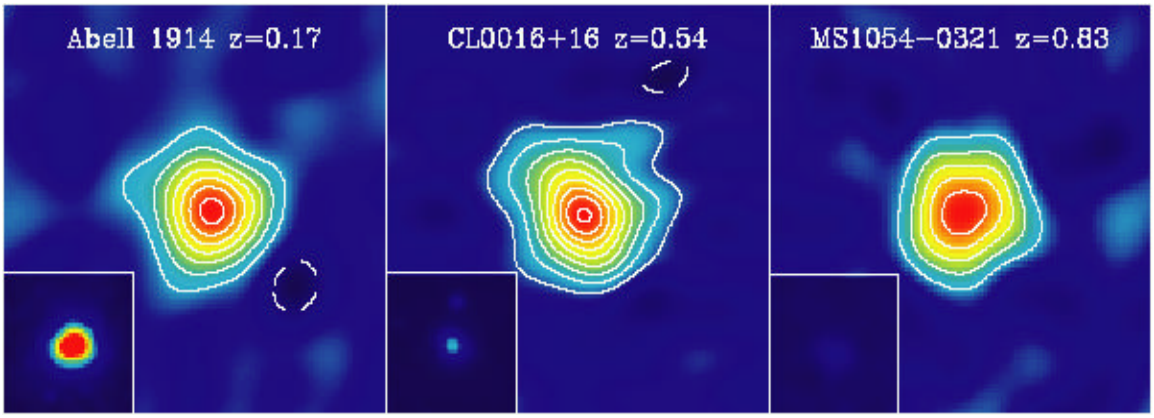

In contrast to x-rays (insets), SZ surface brightness is independent of redshift, so clusters can be seen at any distance.

However, x-ray data needed to determine temperature.

Emerging technique that requires greatly improved arrays.

4. Cryogenic Detector Arrays

Participants in this work (Physics Dept, UCB and LBNL):

John Clarke
Jan Gildemeister *
W. Holzapfel
Trevor Lanting
Adrian Lee
Mike Myers
Paul Richards
Eva Rittweger
H.S.
Jongsoo Yoon**

* now in private industry
** now at Univ. of Virginia

Outline:

1. Why?
2. Transition-Edge Sensors
   - Principles
   - Technology
3. Multiplexers
4. Challenges

Detector Sensitivity

Reminder: Detection threshold in ionization detectors,
e.g. semiconductor detectors

a) visible light (energies near band gap)

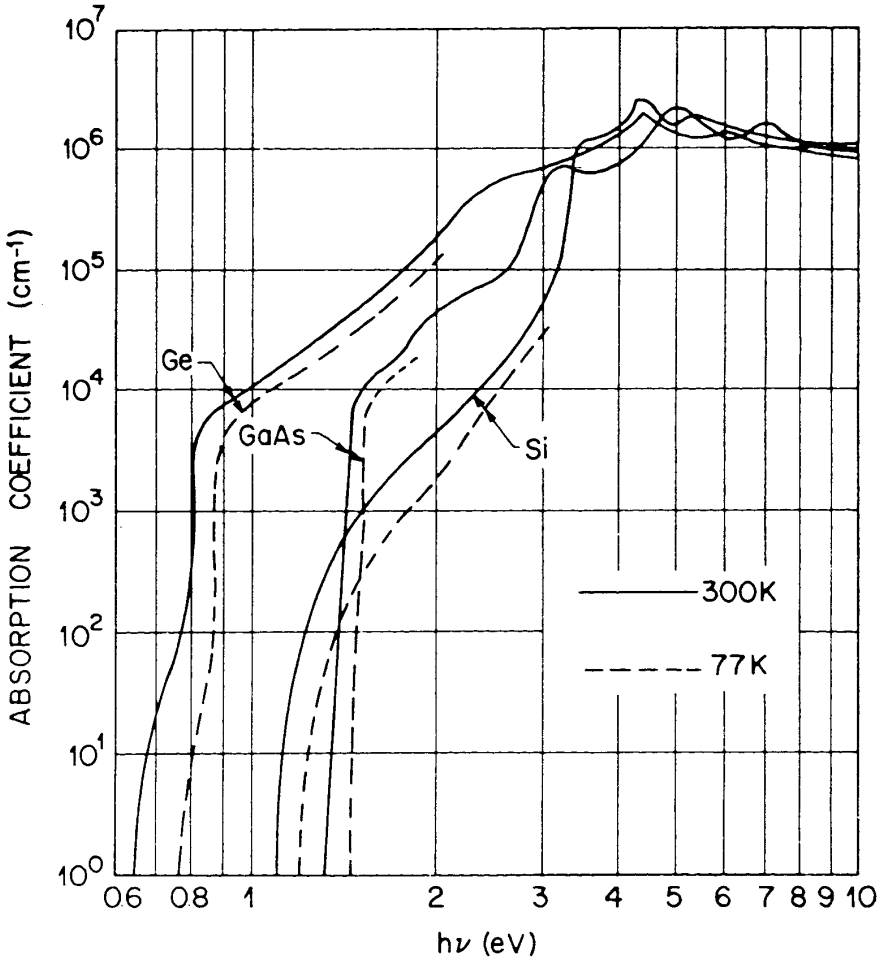

(from Sze)

Detection threshold = energy required to produce an electron-hole pair ≈ band gap

In indirect bandgap semiconductors (Si), additional momentum required: provided by phonons

b) high energy quanta ($E \gg E_g$)

It is experimentally observed that the energy required to form an electron-hole pair exceeds the bandgap.

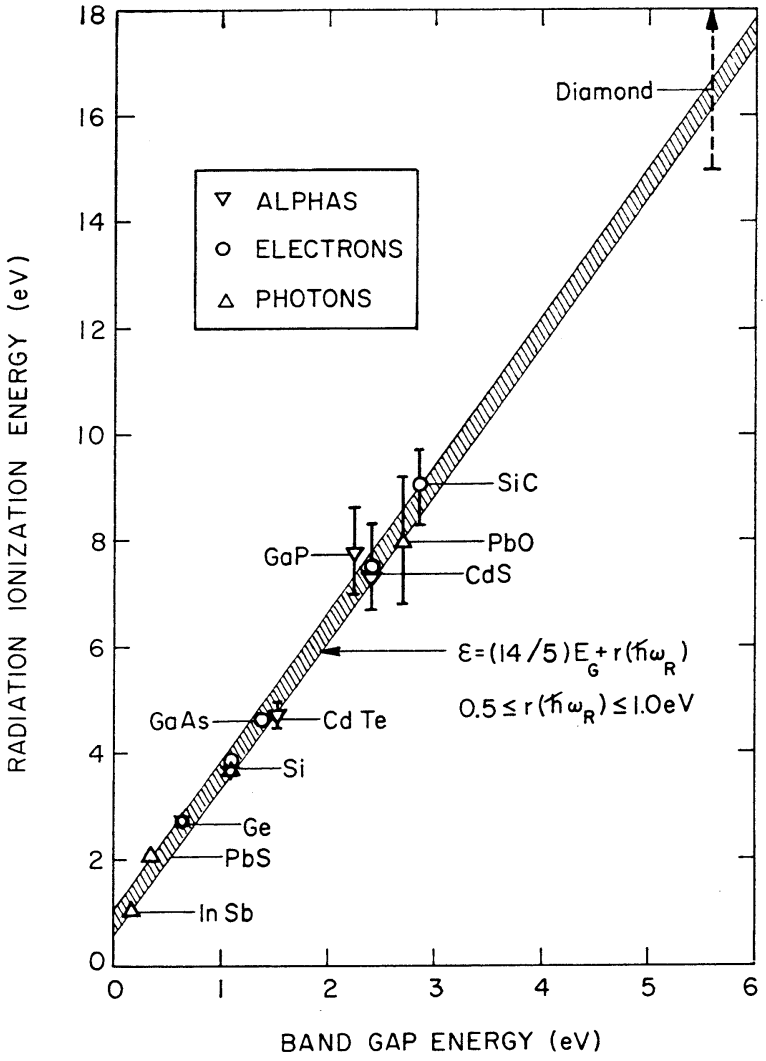

C.A. Klein, J. Applied Physics **39** (1968) 2029

Why?

When particle deposits energy one must conserve both energy and momentum

momentum conservation not fulfilled by transition across gap

⇒ excite phonons

Phonon energy vs. momentum (wavevector k)

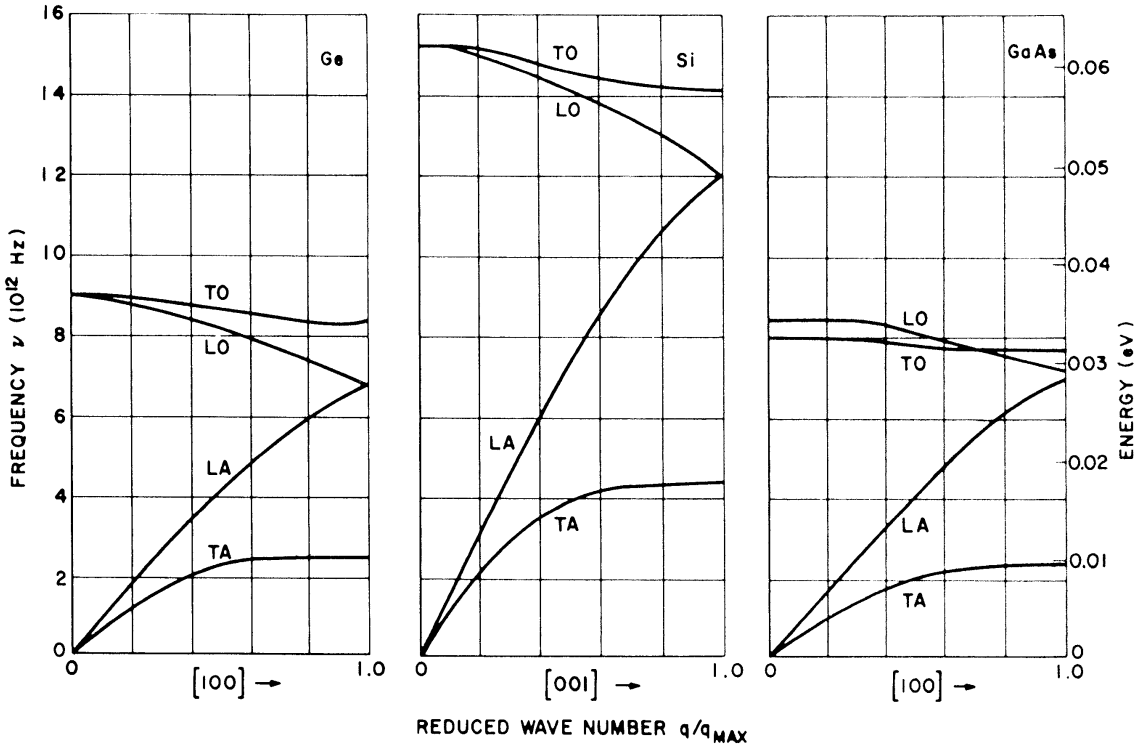

In a semiconductor ionization detector ~60% of the deposited energy goes into phonon excitation.

Instead of detecting electron-hole pairs, detect heat or phonons

Energy scale: 10 meV

$\Rightarrow$ lower energy threshold

Another possibility: Breakup of Cooper pairs in superconductors

The energy gap 2Δ is equivalent to the band gap in semiconductors.

Absorption of energy $>2\Delta$ can break up a Cooper pair, forming two quasiparticles, which can be detected.

The gap energy is typically of order 1 meV.

Thermal Detectors

Basic configuration:

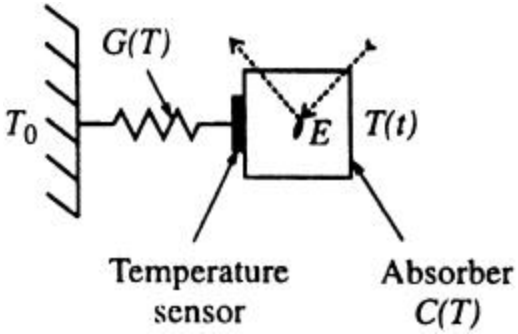

Assume thermal equilibrium:

If all absorbed energy E is converted into phonons, the temperature of the sample will increase by

$$\Delta T = \frac{E}{C}$$

where C the heat capacity of the sample (specific heat x mass).

At room temperature the specific heat of Si is 0.7 J/gK, so

E= 1 keV, m= 1 g $\Rightarrow$ ΔT= $2 \cdot 10^{-16}$ K,

which isn't practical.

What can be done?

a) reduce mass

b) lower temperature to reduce heat capacity
"freeze out" any electron contribution, so phonon excitation dominates.

Debye model of heat capacity: $C \propto \left(\frac{T}{\Theta}\right)^3$

Example: m= 15 µg

T= 0.1 K

Si $\Rightarrow$ C= $4 \cdot 10^{-15}$ J/K

E= 1 keV $\Rightarrow$ ΔT= 0.04 K

How to measure the temperature rise?

Couple thermistor to sample and measure resistance change

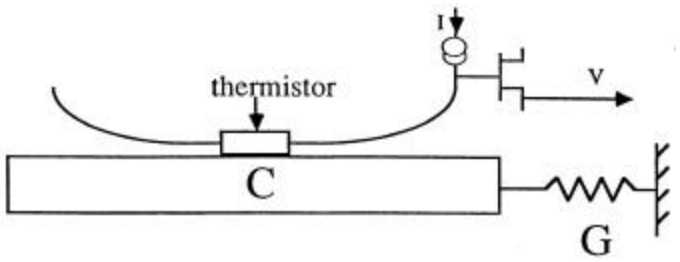

(from Sadoulet at al.)

Thermistors made of very pure semiconductors (Ge, Si) can exhibit responsivities of order 1 V/K, so a 40 mK change in temperature would yield a signal of 40 mV.

Some Old Experimental Results

Monolithic Si calorimeter: 0.25 mm wide x 1 mm long x 15 µm thick
(D. McCammon et al., NIM A326 (1993) 157-165)

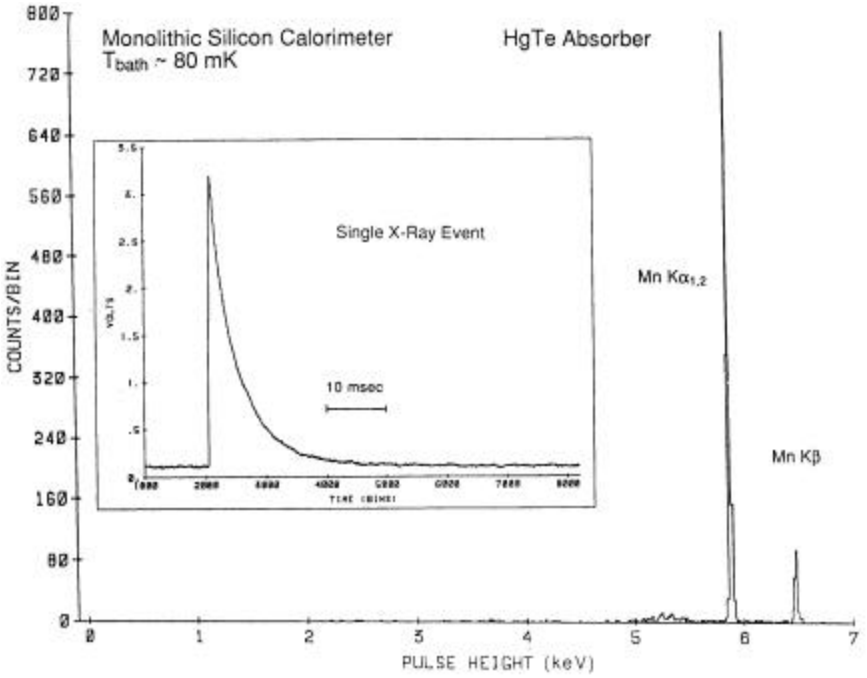

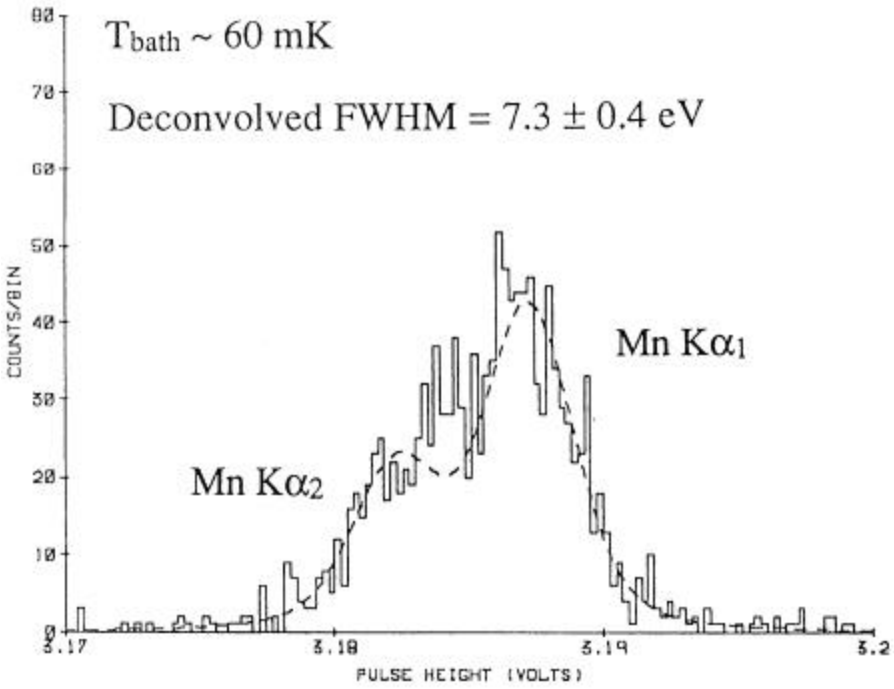

Noise optimization

Absorber coupled to cold finger through thermal conductance G.

The signal pulse will rise rapidly by ΔT and decay exponentially

$$T(t) = \Delta T e^{-t/t}$$

with the decay time

$$t = \frac{C}{G}$$

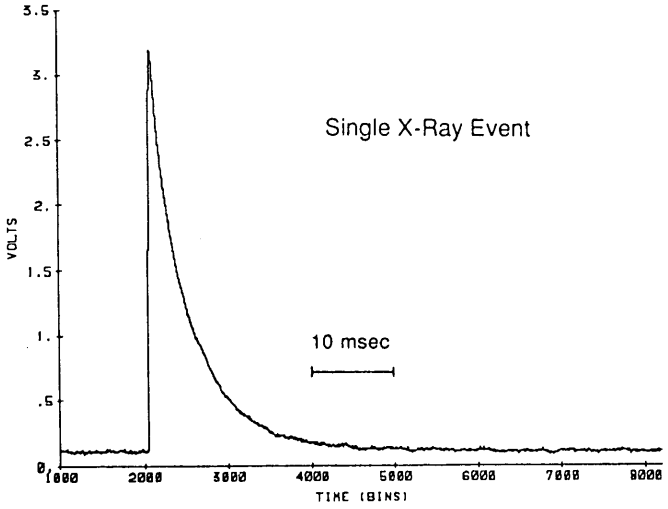

Fluctuations in the phonon number in the absence of incident radiation will give rise to noise pulses with the same shape.

- both the signal and the noise have the same frequency spectrum
- S/N *of sensor alone* is independent of shaping time

However, this does not apply to external noise sources, for example

- resistive sensor
- input transistor
- noise induced by mechanical vibrations

Ideally, front-end and shaper designed to contribute negligible noise, while providing suppression of low-frequency pickup.

Furthermore, phonon fluctuations are increased by fluctuations in signal going into ionization and ionization losses (e.g. trapping).

Transition Edge Sensors

Utilize abrupt change in resistance in transition from superconducting to normal state

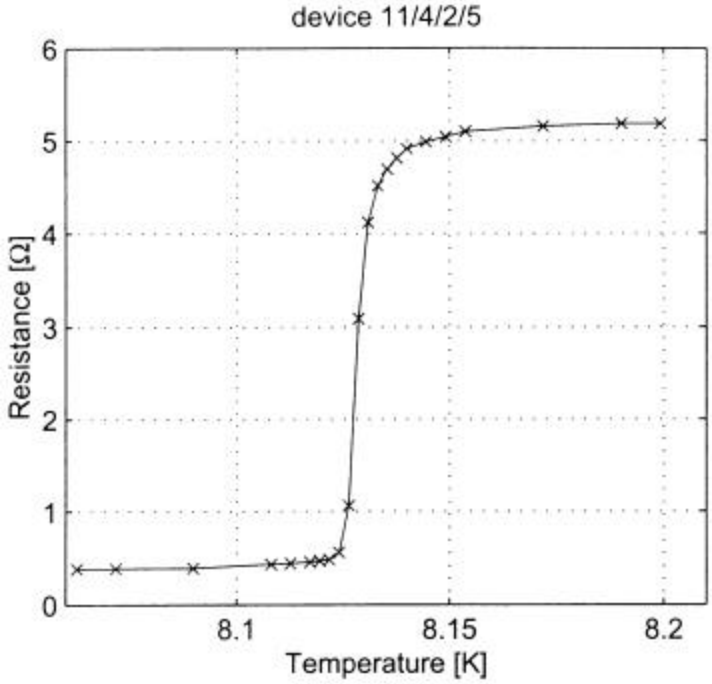

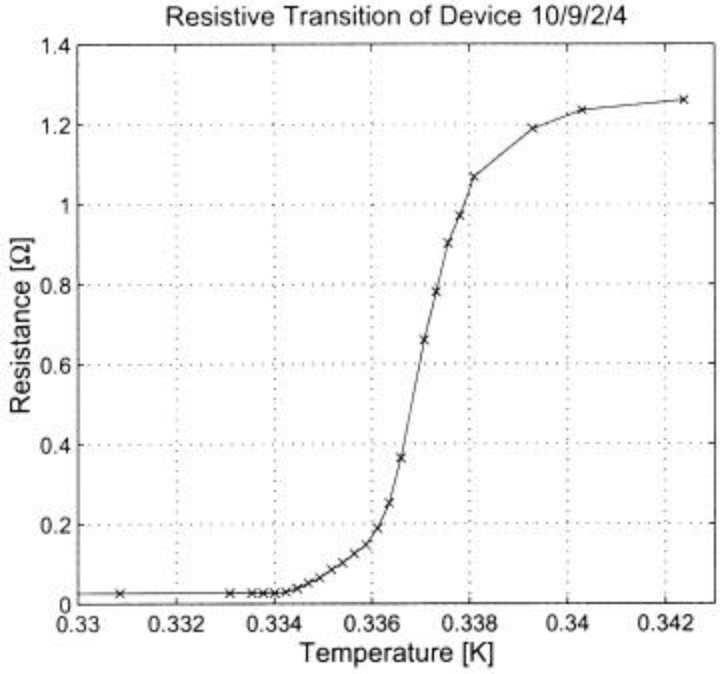

from Jan Gildemeister

Heat Capacity

Insulators

No conduction electrons

$\Rightarrow$ heat capacity due to phonon excitation alone.

$$C(T) = 1944 \frac{m}{M} \left(\frac{T}{\Theta} \right)^3 \ \text{JK}^{-1}$$

where *m* is the mass of the absorber, *M* its molecular weight and Θ the Debye temperature.

Normal metals

heat capacity dominated conduction electrons.

$$C(T) = g\,T$$

Superconductors

Electronic contribution modified by by the presence of the energy gap

$$C \propto \exp(-T_C / T)$$

At sufficiently low temperatures $T \ll T_C$:

Electronic contribution negligible

Heat capacity is the same as for insulators.

Signal Fluctuations

a) Ionization Detector

The statistical fluctuation of a detector signal

$$\frac{s_E}{E} = \sqrt{\frac{F}{N}} = \sqrt{F\frac{e_x}{E}}$$

F is the Fano factor (≈ 0.1 in Si)

Fluctuations increase with $\sqrt{E}$ and decrease with the energy e_x required to form the signal quanta.

b) Thermal Detector

Number of phonon modes excited at temperature T

$$N_{phonon} = \frac{C(T)}{k}$$

and the energy per mode $e_{phonon} = kT$.

Fluctuation in total thermal energy

$$s_0 = e_{phonon}\sqrt{N_{phonon}} = kT\sqrt{\frac{C(T)}{k}}$$

$$s_0 = \sqrt{kT^2C(T)}$$

If an energy quantum E is absorbed into phonon modes, the fluctuation in the number of excited phonons

$$s_E = e_{phonon}\sqrt{\frac{E}{e_{phonon}}} = \sqrt{e_{phonon}E}$$

$$s_E = \sqrt{kTE}$$

The total fluctuation

$$s^2 = s_0^2 + s_E^2 = kT^2C(T) + kTE$$

$$s^2 = kT\left[TC(T) + E\right]$$

Example:

square silicon absorber 0.5 mm on a side and 25 μm thick

heat capacity: $4\cdot10^{-15}$ JK^{-1} at T = 0.1 K.

Then $TC(T) = 4\cdot10^{-16}$ JK^{-1}, which corresponds to E = 2.5 keV.

For T= 0.1 K and C= 4·10^{-15} J/K

$$s_0 = 0.15\ \text{eV}$$

For comparison:

Theoretical limit of Si ionization detector at 1 keV: ~20 eV rms

Worldwide activity on cryogenic detectors has led to impressive results, but devices have been

Hand-crafted

Critical to operate

$\Rightarrow$ only small arrays have been used

Recent developments have changed this picture:

1. Voltage-Biased Transition Edge Sensors

   $\Rightarrow$ stable and predictable response

2. TES can be monolithically integrated using fabrication techniques developed for Si integrated circuits and micromachining.

   $\Rightarrow$ fabricate large arrays with uniform characteristics

Voltage-Biased Transition-Edge Sensors

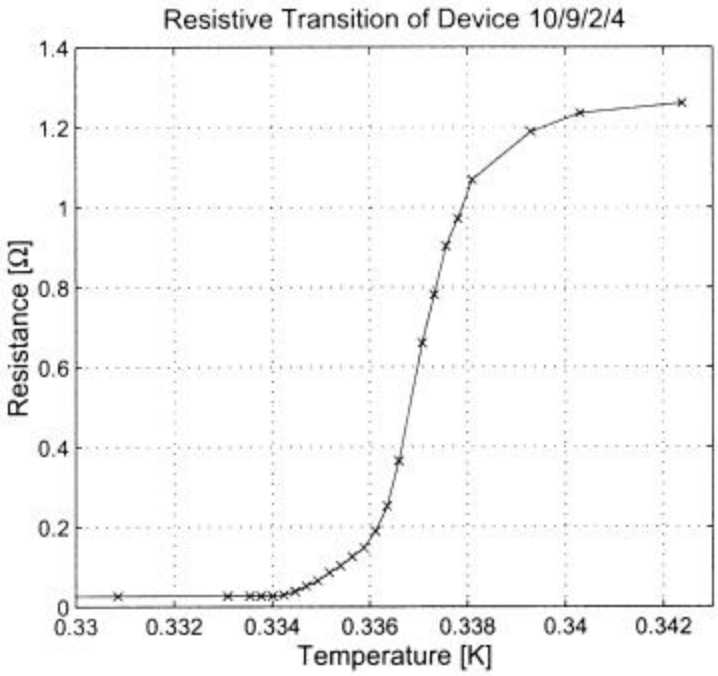

Required power is of order pW, i.e.

voltage of order μV
current of order μA

Simplest to bias device with a constant current and measure change in voltage

Problem: power dissipated in sensor

$$P = I^2 R$$

Increasing $R \Rightarrow$ Increasing $P \Rightarrow$ Increasing $R \Rightarrow$ Increasing P

$\Rightarrow$ thermal runaway

When biased with a constant voltage

$$P = \frac{V^2}{R}$$

Increasing R $\Rightarrow$ Decreasing P $\Rightarrow$ Decreasing T $\Rightarrow$ Decreasing R

$\Rightarrow$ **negative feedback**

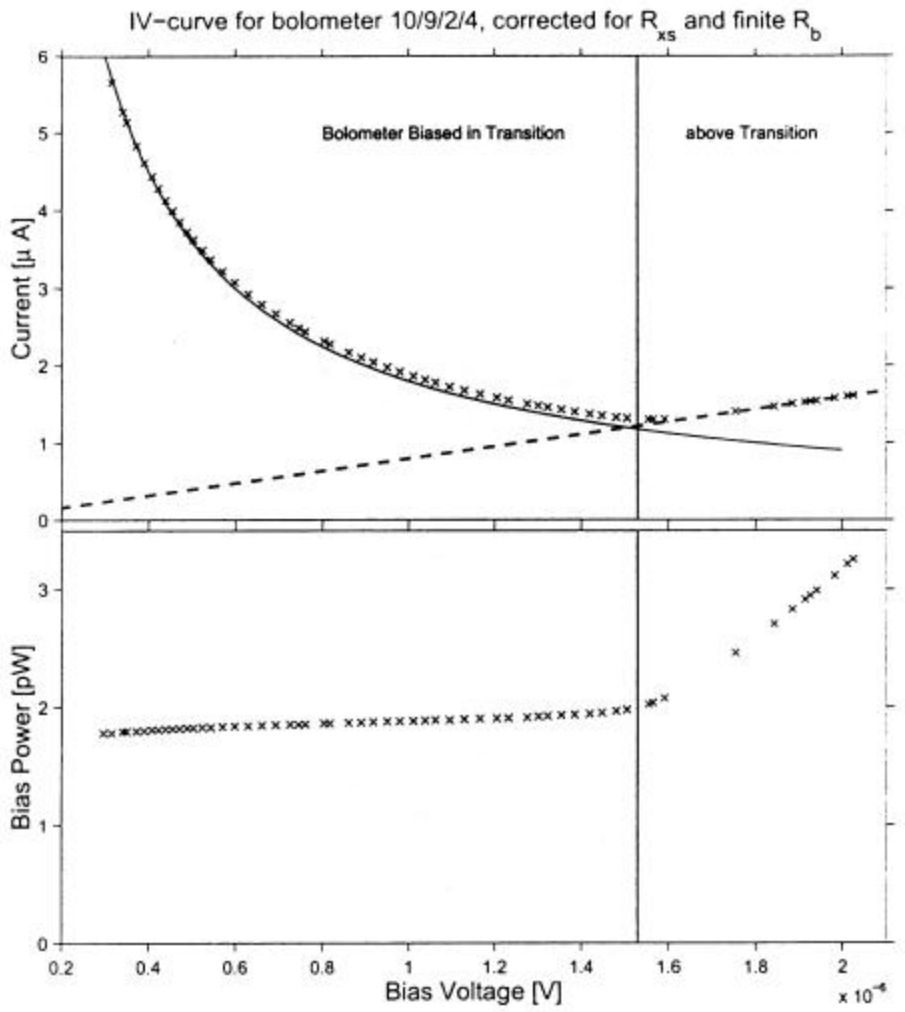

from Gildemeister

In the transition regime the power is roughly independent of bias voltage.

In the presence of electrothermal feedback the detector response

$$T = \frac{\Phi_0 t}{C}\left(1 - e^{-t/t}\right)$$

where Φ_0 is the incident signal and the time constant t

$$t = \left(\frac{a V^2}{R_0 T_0 C} + \frac{G}{C}\right)^{-1} = \frac{C/G}{1 + \frac{a V^2}{R_0 T_0 G}}$$

The parameter α characterizes the dependence of resistance on temperature

$$a = \frac{d(\log R)}{d(\log T)}$$

For negligible feedback

$$\frac{a V^2}{R_0 T_0 G} \ll 1$$

and the decay time constant

$$t = \frac{C}{G}$$

is the natural time constant given by the heat capacity C and thermal conductance G .

- Substantial feedback reduces the response time (as in op-amps).

The change in current for a short pulse with thermal energy Q_0

$$I(t) = -\frac{a\,V}{R_0 T_0}\frac{Q_0}{C}e^{-t/t}$$

For large negative feedback

$$\frac{R_0 T_0 G}{V^2 a} \ll 1$$

and

$$Q_0 = -V\int_0^\infty I(t)dt$$

$\Rightarrow$ calibration is determined only by magnitude of bias voltage.

Important constraint:

Since sensor resistance of order 0.1 – 1 Ω, the total external resistance, i.e.

- Internal resistance of voltage source
- Input resistance of current measuring device

must be much smaller to maintain voltage-biased operation, i.e. < 0.01 – 0.1 Ω !

Difficult to achieve at relevant frequencies.

Solution: SQUID readout

SQUIDs are good match for TES readout

- low temperature device
- very low noise possible
  (10 mK noise temperature compared to sensor temperature of 100 – 300 mK)
- low input impedance (input inductance ~100 pH)
- adequate gain to drive room-temperature amplifier without significant noise degradation

However,

- Input signal may not exceed 1/4 flux quantum
  (output periodic in Φ_0)
- Feedback loop required to lock flux at proper operating point
  (flux locked loop)

Results from NIST group, using transition edge sensors
With SQUID readout (Martinis et al.)

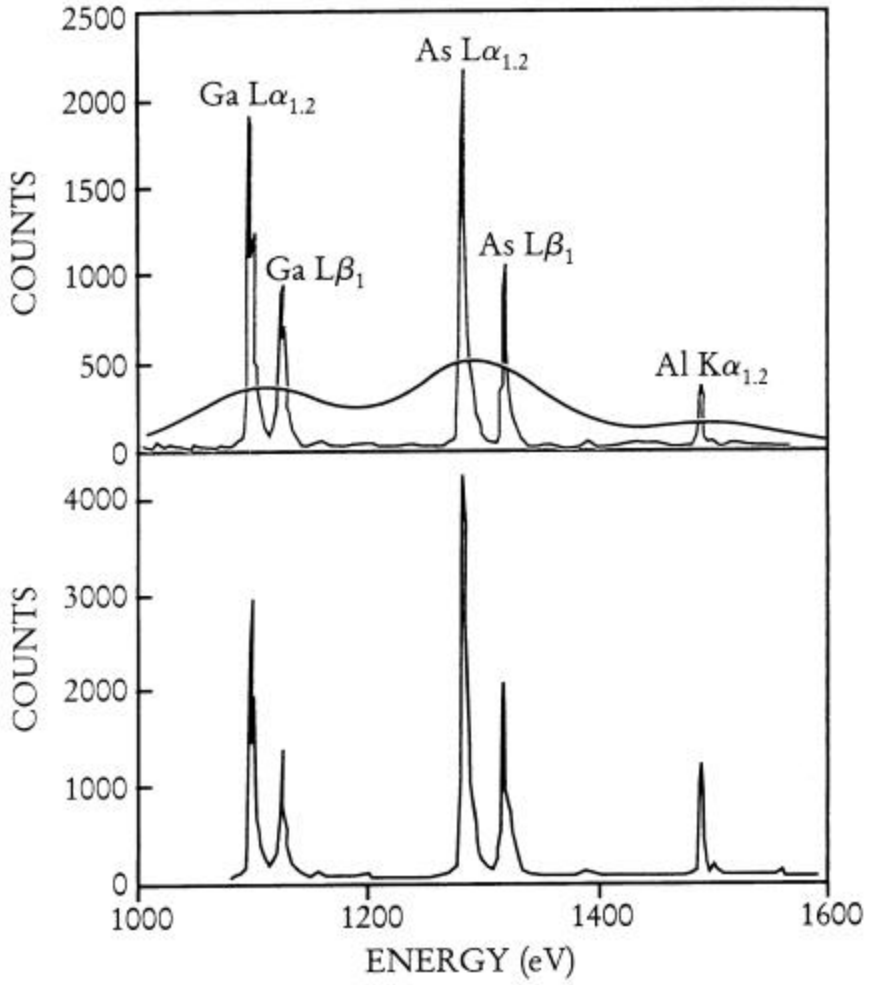

Upper plot: microcalorimeter spectrum (4 eV resolution) with superimposed spectrum from conventional Si detector

Lower plot: crystal diffraction spectrometer

Monolithic Fabrication of TES Arrays

(Jan Gildemeister et al.)

TES sensor can be fabricated with thin film deposition.

Signal is captured by metallic grid on Si-nitride beams
(7 μm wide x 1 thick)

Sensor in middle of grid: Ti (500Å) – Al(400Å) – Ti(500Å) – Al(1000Å)
(dot in middle of lower figure)

Prototype 32 x 32 Si_2N_3 array:

Grid made from film oflow-stress Si-nitride etched to form beams.

Connected to frame at 4 points (arrows)

- high thermal resistance
- connections to readout

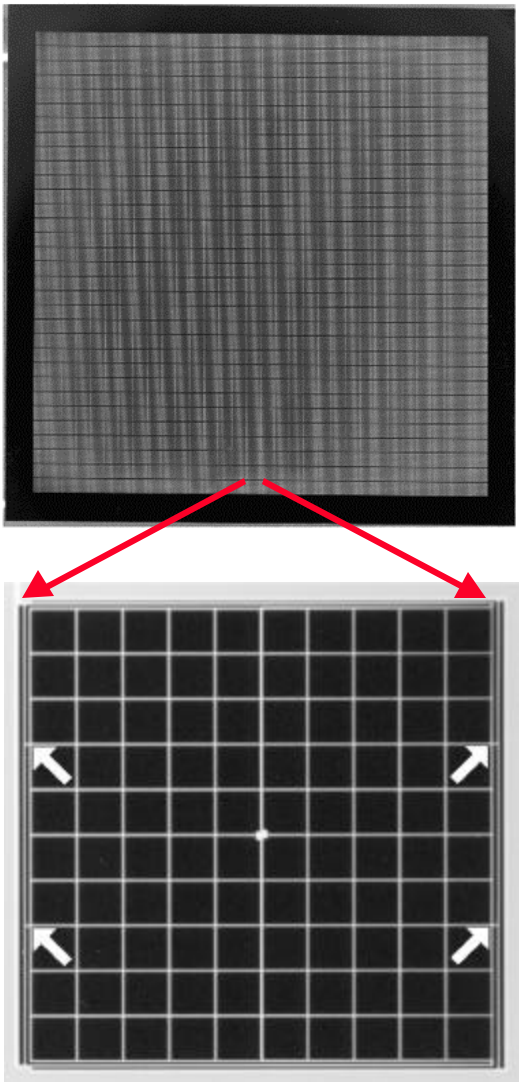

Single pixel:

1.5 mm

1.5 mm

Cross Section of Pixel

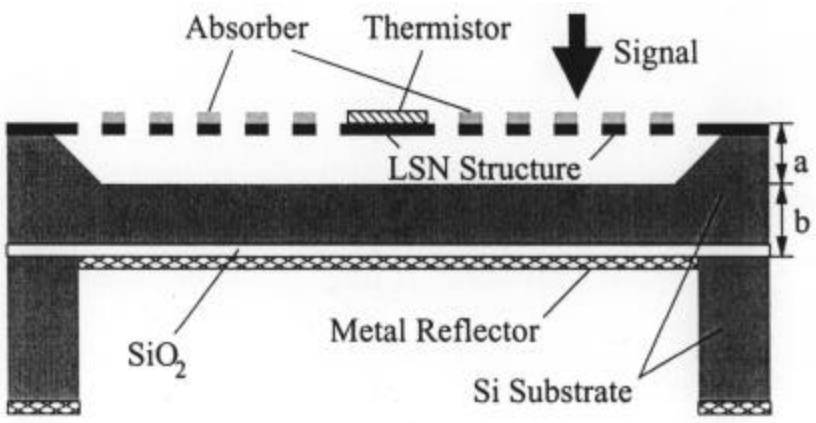

Etch detail

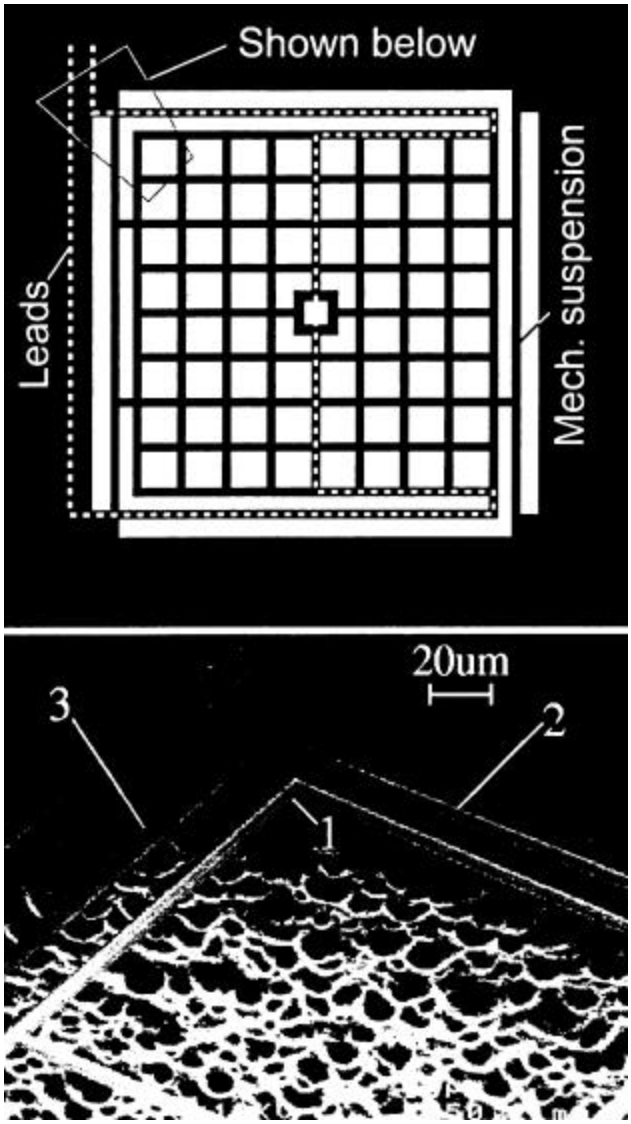

Transition temperature is adjusted by choice of thickness and materials in sensor sandwich:

1. Transition temperature depends on film thickness

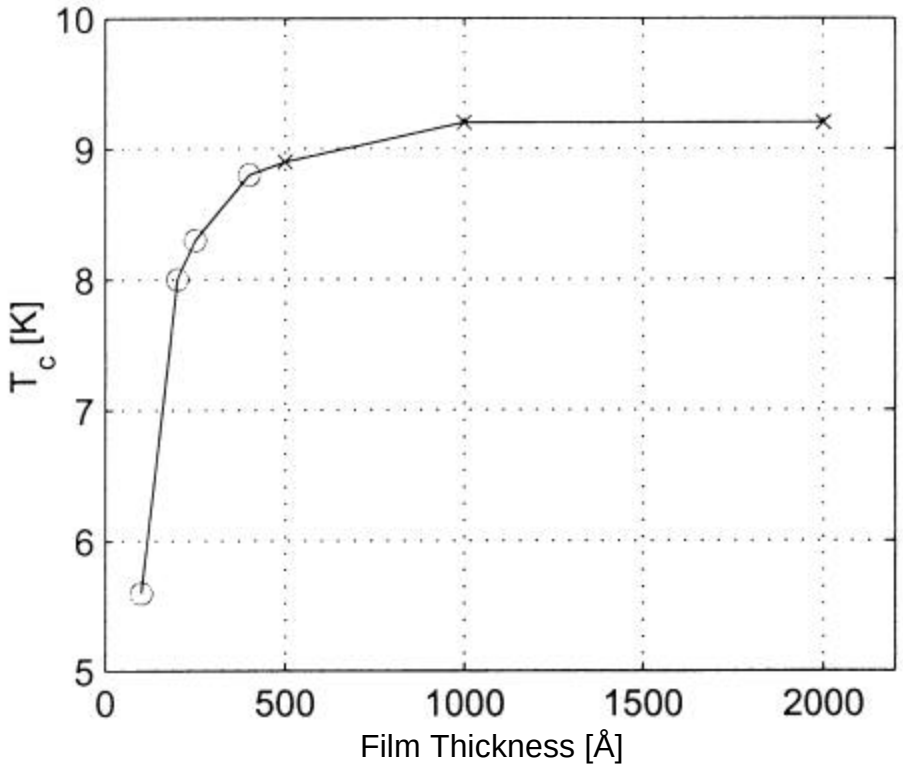

Jan Gildemeister

2. Thin adjacent layers interact ("Proximity Effect")

Measured Noise

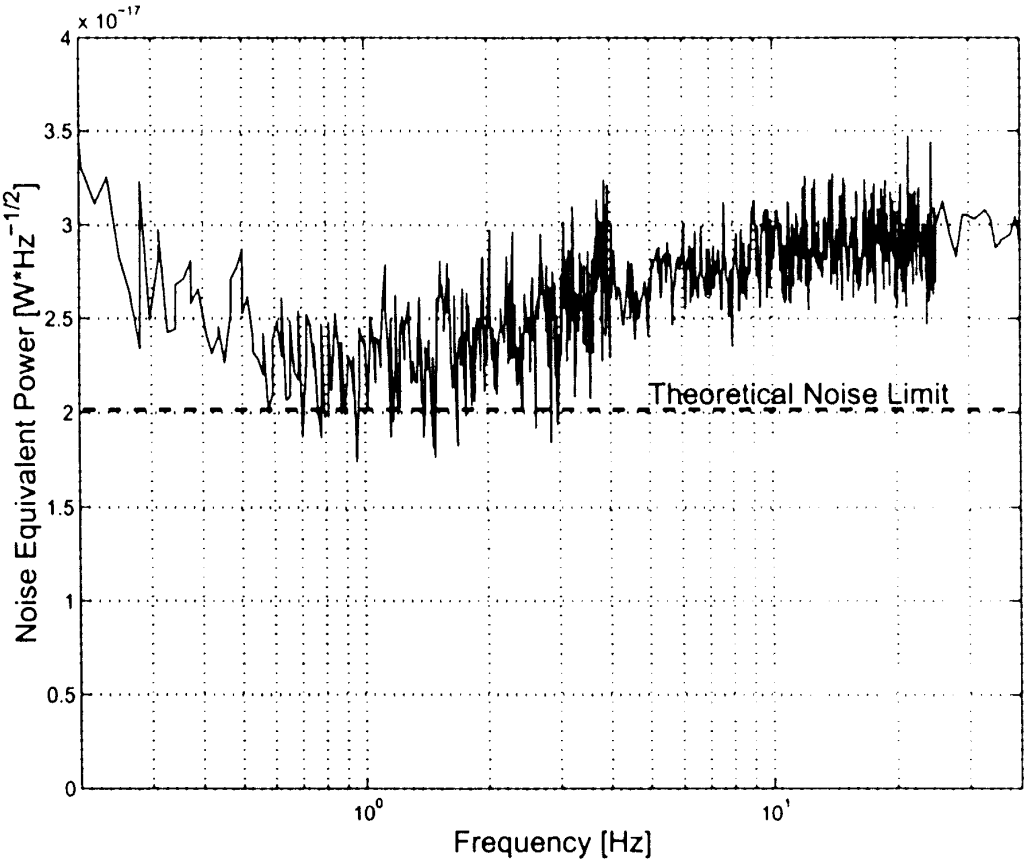

Jan Gildemeister

Integrate Antennas + Bandpass Filters + Sensors
(Mike Myers)

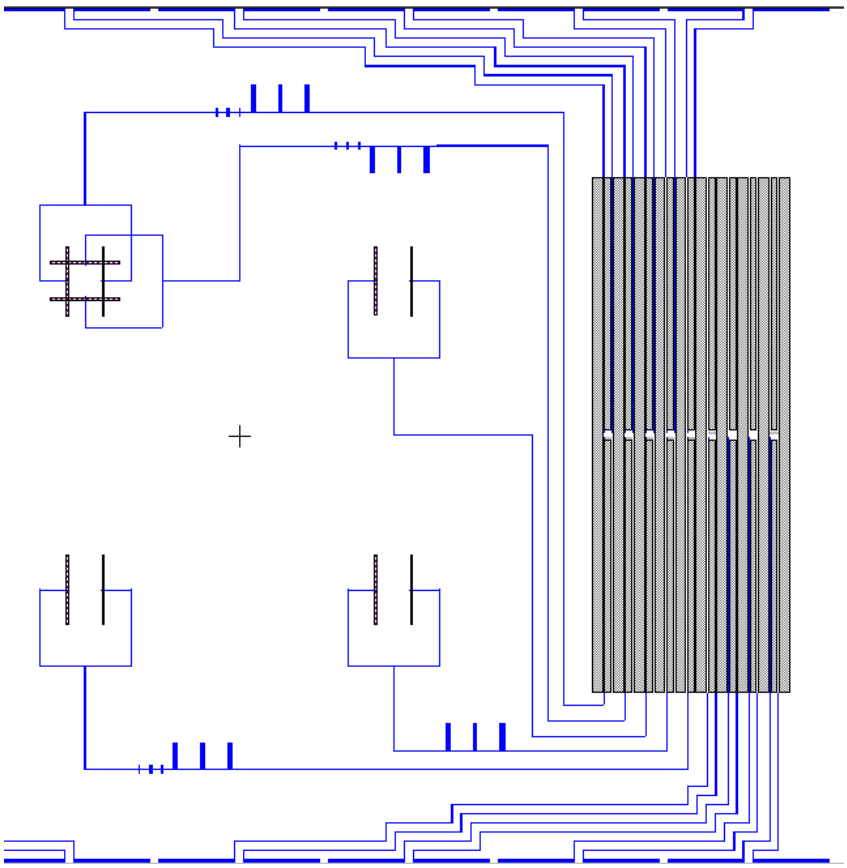

Utilize alternative sensor design

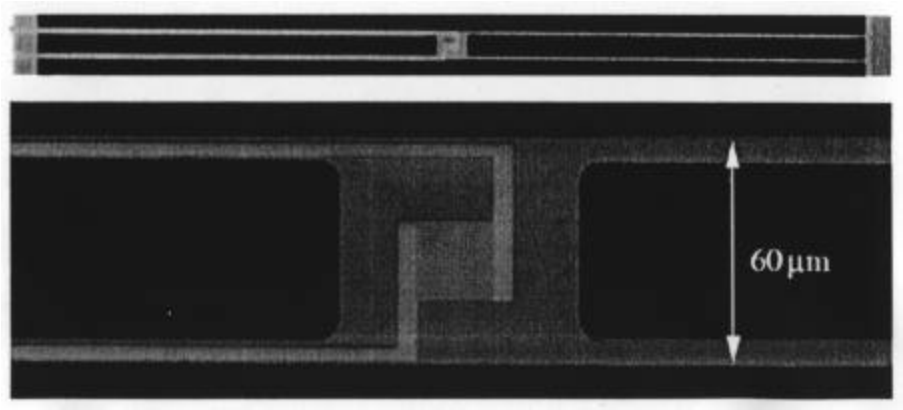

Readout

How to read out thousands of sensors?

1. Time Domain Multiplexer (NIST): use 1 SQUID switch per sensor

2. Frequency Domain Multiplexer (Berkeley):
1 SQUID per ~30 sensors

Frequency Domain Multiplexer

- Sensors biased with high-frequency signal (100 kHz – 1 MHz)
- When signal power is absorbed, resistance changes and current is modulated by signal.
- Each sensor is biased at a separate frequency.
- Multiple sensor outputs can be summed and read out by single SQUID
- External frequency-selective demodulators extract signal

Modulation Basics

If a sinusoidal current $I_0 \sin wt$ is amplitude modulated by a second sine wave $I_m \sin w_m t$

$$I(t) = (I_0 + I_m \sin w_m t)\sin wt$$
$$I(t) = I_0 \sin wt + I_m \sin w_m t \sin wt$$

Using the trigonometric identity $2 \sin a \sin b = \cos(a - b) - \cos(a + b)$ this can be rewritten

$$I(t) = I_0 \sin wt + \frac{I_m}{2}\cos(wt - w_m t) - \frac{I_m}{2}\cos(wt + w_m t)$$

The modulation frequency is translated into two sideband frequencies $(wt + w_m t)$ and $(wt - w_m t)$ symmetrically positioned above and below the carrier frequency w.

All of the information contained in the modulation signal appears in the sidebands; the carrier does not carry any information whatsoever.

The power contained in the sidebands is equal to the modulation power, distributed equally between both sidebands.

Although the phase of the modulation signal is not correlated with the carrier, there is a fixed phase relationship between the sidebands and the carrier.

If the signal is modulated by noise, the spectral components of the noise signal have a random phase with respect to one another, but the two sideband spectra have a fixed 180° phase shift with respect to one another and a 90° phase shift with respect to the carrier.

Signal Summing Schemes

a) Voltage Summing

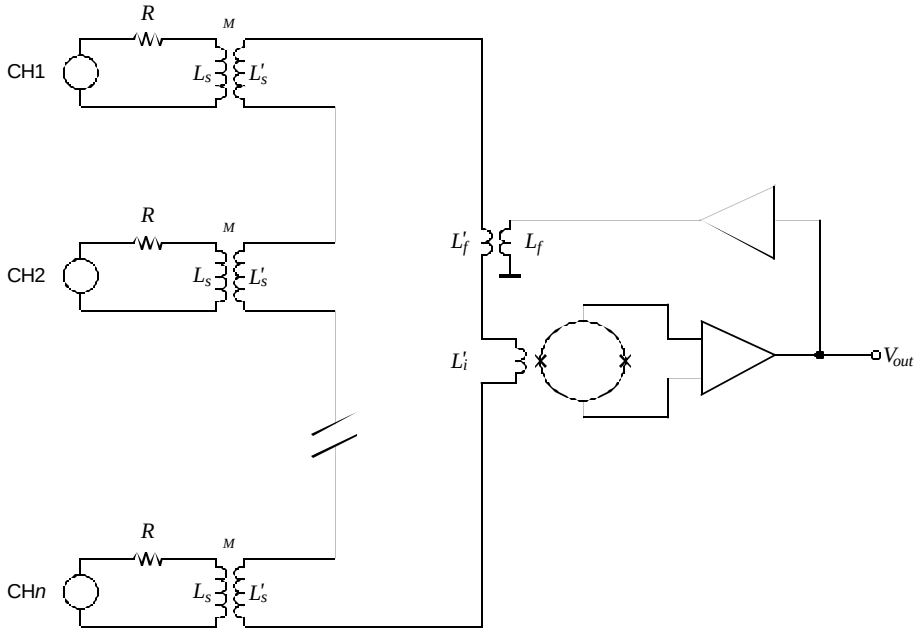

b) Current Summing

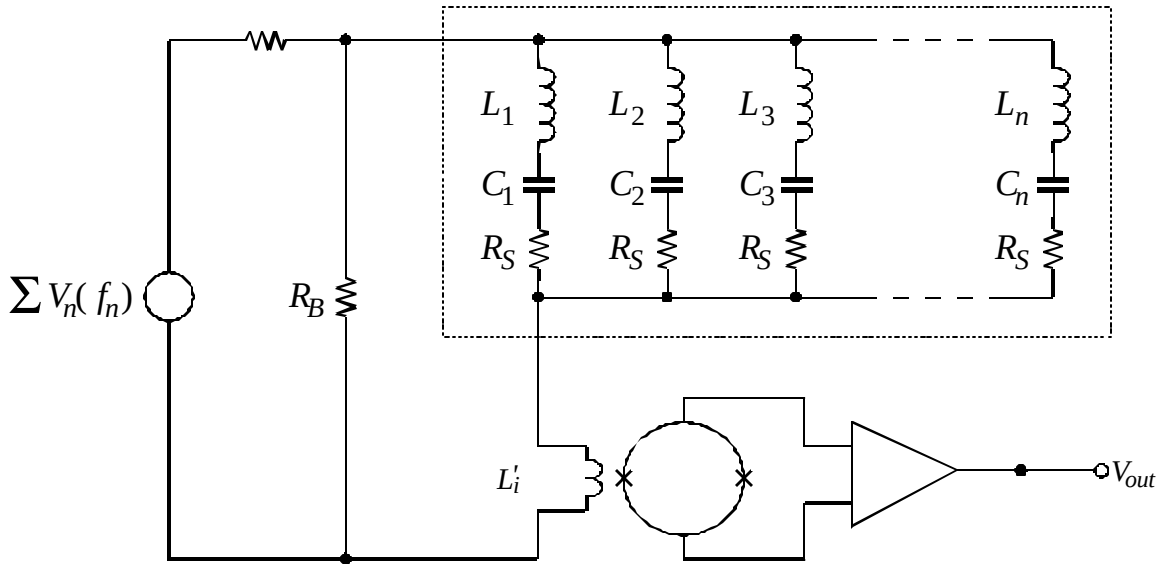

1. The sensors are AC biased by the frequency generator at the left of the figure. The AC drive signal is applied as a comb spectrum $V(t) = \sum V(f_n) = \sum V_n \cos(w_n t)$. The bias resistance R_B is much smaller than the sensor resistance R_S to ensure voltage-biased operation.

2. The individual series resonant circuits $L_n C_n$ are set to the component frequencies of the drive spectrum, so that each leg of the sensor array is driven predominantly by only one frequency f_n.

3. Signal power absorbed by the sensor modulates the current flow through the tuned circuit, translating a signal spectrum Δf_s into sidebands $f_n \pm \Delta f_s$ above and below the corresponding carrier frequency.

4. The sum of all sensor currents is sensed by an output current amplifier.

   Its input impedance must be much smaller than the sensor resistance over the whole range of bias frequencies, again to ensure voltage-biased operation.

5. A bank of frequency-selective demodulators extracts the individual signals from the composite signal.

Cross-Talk

Selectivity of tuned circuits attenuates carrier currents flowing into "wrong" channels

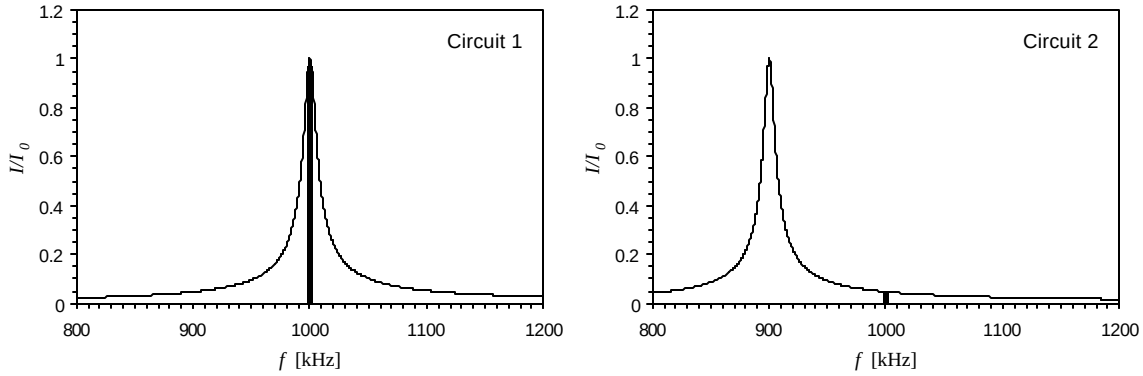

Current of a given frequency flows through the neighbor channel and introduces signal components from the that channel.

The thick vertical lines indicate the relative magnitude of the carrier current.

Circuit 1 resonates at the carrier frequency, so the current is maximum.

Circuit 2, the neighbor channel, resonates at 900 kHz, so the 1000 kHz carrier current is smaller.

The curves are for a *Q* of 100 and the current through the neighbor channel is 5% of the maximum.

Cross-Coupling of Noise

1. Each sensor generates a wideband noise spectrum, shaped by the selectivity curve of the corresponding tuned circuit. Thus, noise from all sensors appears at a given channel frequency.

2. The fractional carrier of frequency f_n flowing through the neighbor channels $f_{m \neq n}$ is modulated by the sensor noise and adds to the total noise in the sidebands associated with f_n . The relative magnitude of this contribution is determined by the cross-talk, as was illustrated on the previous slide.

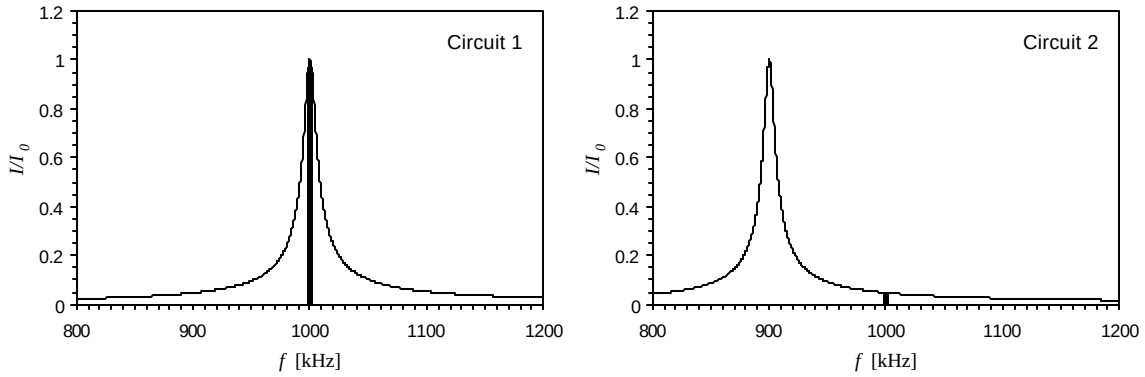

Wideband noise is generated by all of the sensor resistances and filtered by the selectivity of the associated tuned circuits.

At resonance (left, circuit 1) the full noise power appears in the passband surrounding the 1000 kHz carrier frequency (represented by the thick vertical line).

Noise originating in circuit 2 (right) also appears in the passband at 1000 kHz, but is attenuated.

Demodulation

The same carrier signal that biases the sensor is used to translate the sideband information to baseband.

The mixer acts analogously to a modulator, where the input signal modulates the carrier, forming both sum and difference frequencies.

In the difference spectrum the sidebands at $f_n \pm \Delta f_S$ are translated to a frequency band $f_n - (f_n \pm \Delta f_S) = 0 \pm \Delta f_S$.

A post-detection low-pass filter attenuates all higher frequencies and determines the ultimate signal and noise bandwidth.

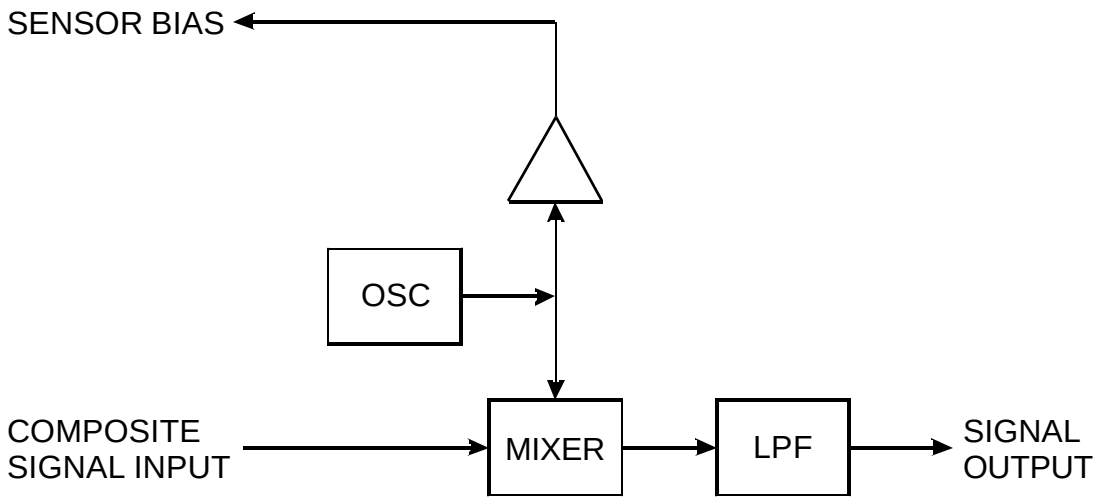

Demodulator Bank per 30-ch Sensor Module

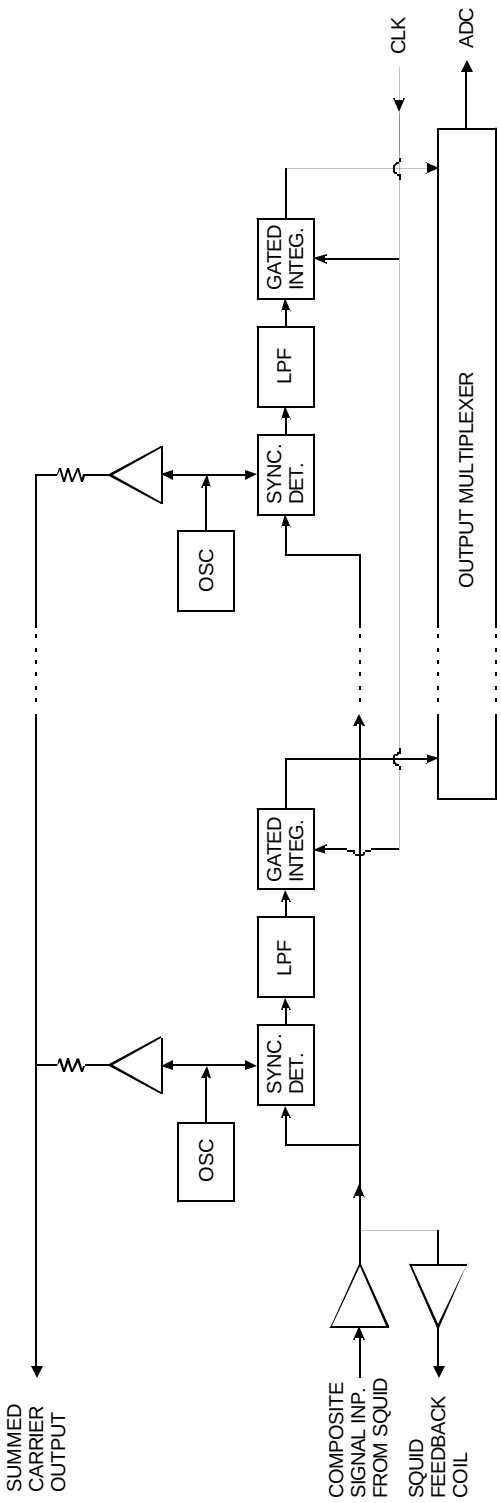

Some Challenges

1. Dynamic Range of SQUID

SQUID limits maximum signal to $\Phi_0/4$.

Since carrier amplitudes are much larger than noise, the combined carrier signal can exceed the maximum signal level of the SQUID.

Optimized feedback loop can extend dynamic range by >10 relative to current systems, but this may not be enough.

Since the carrier carries no information, it can be attenuated.

Introduce carrier component with opposite phase at summing junction (carrier nulling).

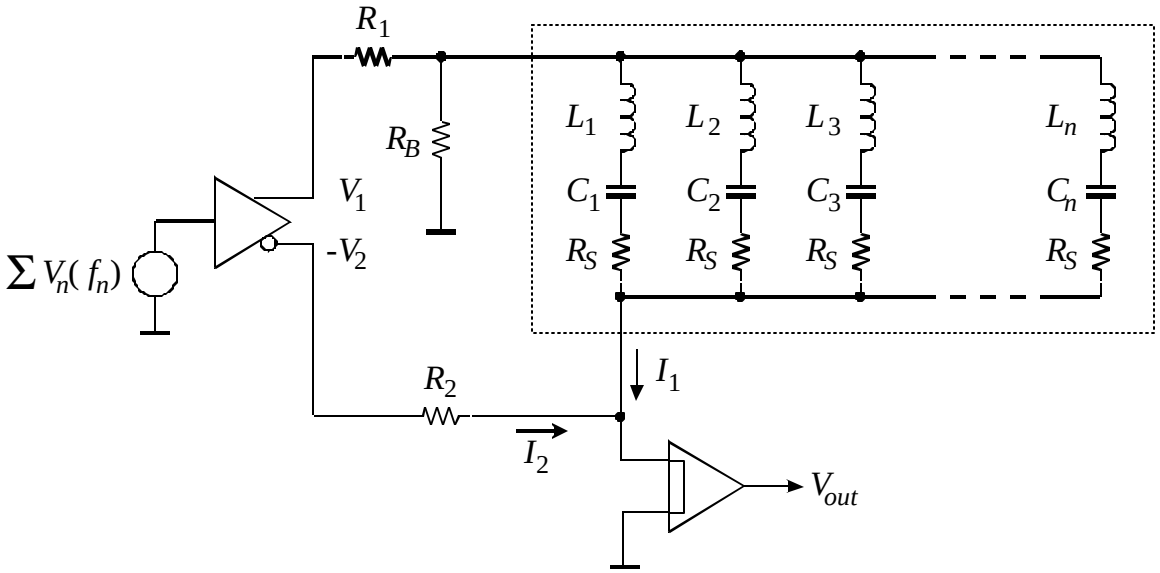

Phase shift in tuned circuits changes maximally with frequency at resonance.

$\Rightarrow$ frequency must be settable and controlled accurately

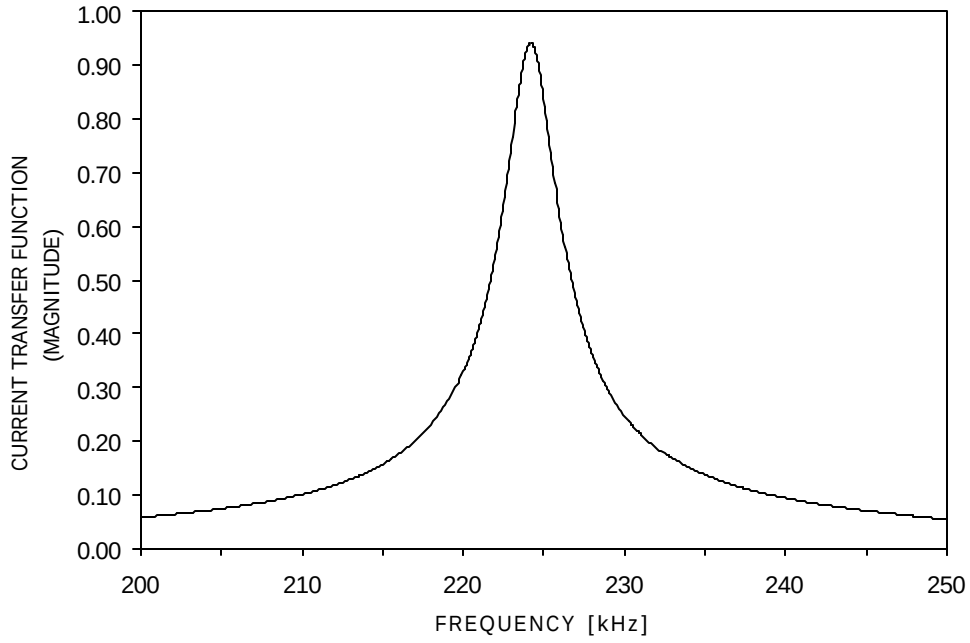

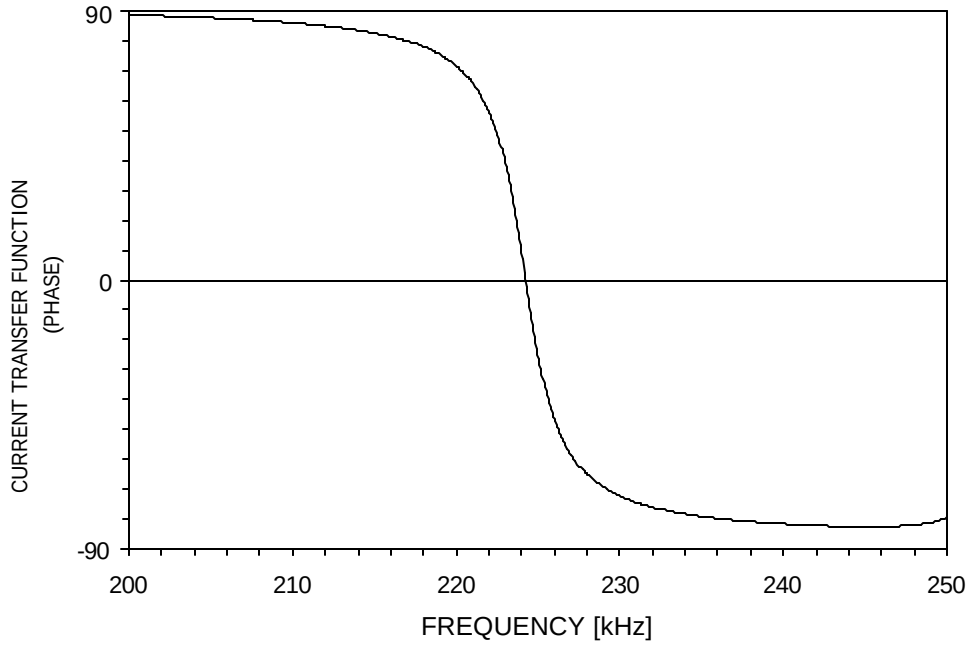

2. Carrier Noise

TES is biased by an AC current, which is modulated by the signal.

The ultimate detection limit is determined by the thermodynamic noise of the sensor and the thermal noise associated with its resistance.

$$P_N = 4kT_S b + \sqrt{4kT_S^2 Gb}$$

where *b* is the noise bandwidth.

The sensor noise is distributed into two sidebands. In one sideband the ratio of noise to carrier power

$$\frac{P_N}{P_S} = \frac{1}{2}\frac{4kT_S b + \sqrt{4kT_S^2 Gb}}{V_S^2 / R_S}$$

A typical sensor power is 10 pW. For a noise bandwidth of 1 kHz, an operating temperature T = 0.1 K and a thermal conductance $G = 10^{-10}$ W/K, the noise-to-carrier ratio

$$\frac{P_N}{P_S} = \frac{4kT_S b + \sqrt{4kT_S^2 Gb}}{2P_S} \approx \frac{10^{-16}}{10^{-11}} = 10^{-5} \ ,$$

or –50 dBc (50 dB below carrier). In this example the phonon noise dominates.

Additional noise is introduced by the carrier generator.

The resonator waveform is modulated by the noise of the amplifier device, which causes fluctuations in amplitude, frequency and phase, all of which manifest themselves as noise sidebands.

see Oscillator Phase Noise: A Tutorial, T.H. Lee and A. Hajimiri, IEEE J. Solid State Circuits SC-35/3 (2000) 326 - 336

Since oscillators invariably include some form of amplitude limiting, the frequency and phase modulation are the dominant sources of sideband noise.

Sideband noise is usually expressed per Hz bandwidth, so for a sensor power of 10 pW the noise of the carrier generator at the frequencies of interest must be $\ll 10^{-8}$ = –80 dBc/Hz.

To limit the generator's noise contribution to <10% of the sensor noise, the sideband noise should not exceed –90 dBc/Hz.

The relevant signal spectrum is in the range 0.1 Hz to 1 kHz.

Sideband noise of a high-quality frequency synthesizer:

At frequencies <10 Hz the noise is marginal.

Very high-quality synthesizer:

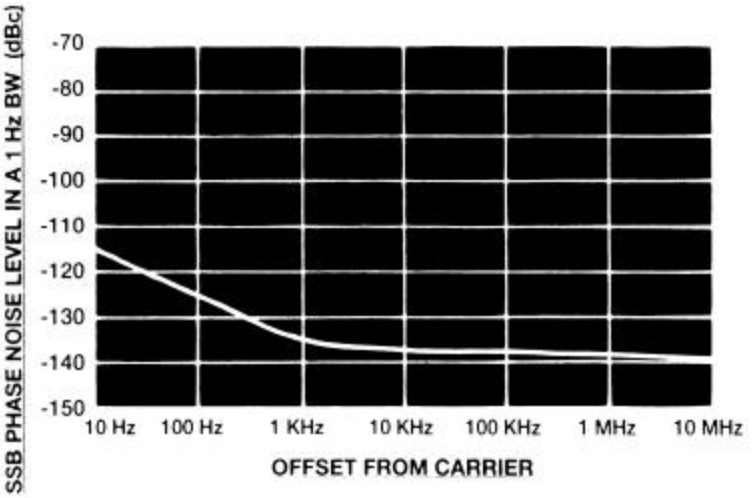

The required oscillator noise level is feasible, but with one programmable oscillator per sensor this has to be done economically.

5. Summary

Breakthrough in Cryogenic detectors

- Sensitivity approaching quantum level at mm wavelengths
- Voltage-biased superconducting transition edge sensors

  ⇒ stable operation
  predictable response

- Sensors can be fabricated using monolithic technology developed for Si integrated circuits, micro-mechanics

  ⇒ economical fabrication of large sensor arrays

- Open question: Readout
  (multiplexing of many channels)

  Appears feasible, but much work to do

- critical for CMB Polarization
  SZ Cluster Search
  Next Generation WIMP detectors

- great opportunities for students + post-docs!

6. Outlook

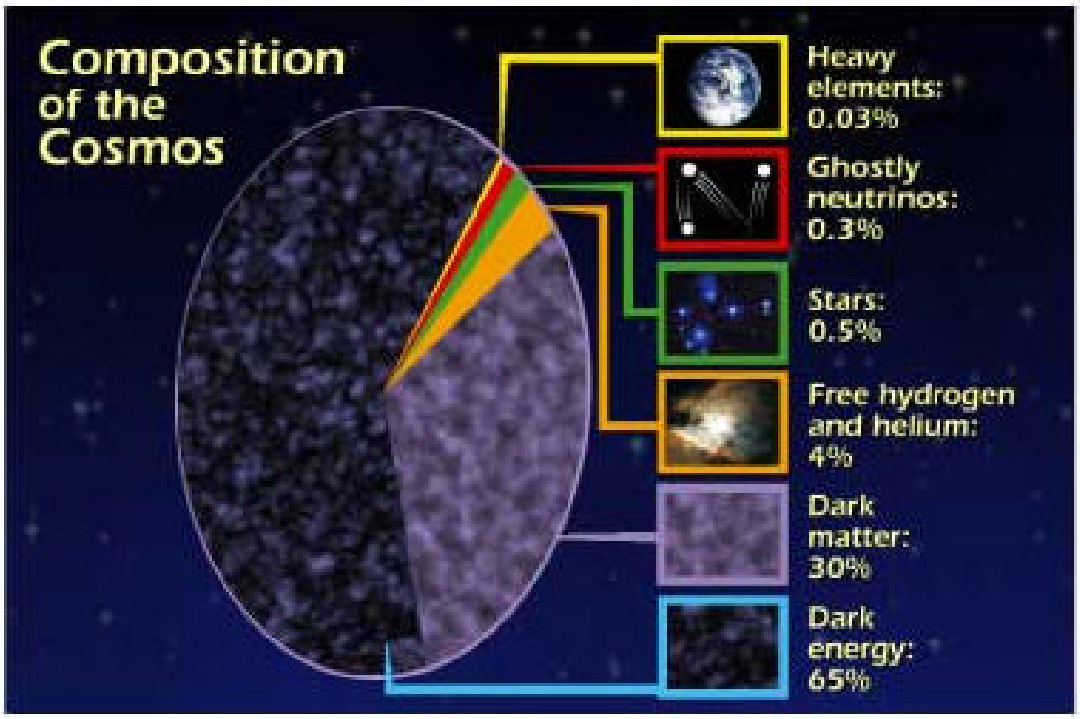

Based on our current data, dark matter and dark energy constitute 95% of the universe.

We don't know what the dark matter is, nor do we have any credible explanation of dark energy.

All of the physics and chemistry of the past ~400 years has been directed at understanding only 5% of the universe!

One thing is clear - detectors and signal processing will play a key role in solving these mysteries.